Published in final edited form as:
Neuron. 2009 June 11; 62(5): 633–640. doi:10.1016/j.neuron.2009.05.016.

The stoichiometry of AMPA receptors and TARPs varies by neuronal cell type

Yun Shi, **Wei Lu**, **Aaron D. Milstein**, and **Roger A. Nicoll***
Departments of Cellular and Molecular Pharmacology and Physiology, University of California San Francisco, California 94143, USA

Summary

Fast synaptic transmission in the brain is mediated by activation of AMPA-type glutamate receptors (AMPARs). AMPARs are comprised of four pore forming subunits (GluAs) as well as auxiliary subunits referred to as transmembrane AMPA receptor regulatory proteins (TARPs). TARPs control the trafficking and gating of AMPARs. However, the number of TARP molecules that assemble within an individual AMPAR complex is unknown. Here, we covalently link GluAs to TARPs to investigate the properties of TARP/AMPAR complexes with known stoichiometry in HEK cells. We find that AMPARs are functional when associated with either four, two, or no TARPs, and that the efficacy of the partial agonist kainate varies across these conditions, providing a sensitive assay for TARP/AMPAR stoichiometry. By comparing these results with data obtained from hippocampal neurons, we show that native AMPARs are normally associated with multiple TARP molecules, and that native TARP/AMPAR stoichiometry varies with the expression level of endogenous and exogenous TARPs. Interestingly, AMPARs in hippocampal pyramidal cells contain more TARP molecules than those in dentate gyrus granule cells, suggesting a cell type-specific regulatory mechanism for TARP/AMPAR stoichiometry.

Introduction

Glutamate, the main fast excitatory neurotransmitter in the CNS, acts primarily on two types of ionotropic receptors: NMDA receptors and AMPA receptors (AMPARs). Activation of AMPARs by synaptic glutamate results in fast moment-to-moment depolarization of postsynaptic neurons, a process crucial for information propagation in the CNS. AMPAR subunits form ion channels by assembling as heterotetramers of GluA1-GluA4 (GluR1-GluR4 or GluR-A – GluR-D) (Collingridge et al., 2008; Dingledine et al., 1999; Hollmann and Heinemann, 1994; Mayer and Armstrong, 2004; Seeburg, 1993). In addition to these principal subunits, native AMPARs also associate with auxiliary subunits known as TARPs (Chen et al., 2000; Nicoll et al., 2006; Osten and Stern-Bach, 2006; Ziff, 2007). There are four classical TARPs in the CNS: γ-2, γ-3, γ-4, and γ-8 (Tomita et al., 2003). These molecules associate with all four GluAs and regulate their trafficking, gating, and pharmacology in a TARP subtype-specific manner (Milstein and Nicoll, 2008; Nicoll et al., 2006; Osten and Stern-Bach, 2006; Ziff, 2007). While most neurons express more than one TARP subtype, cerebellar granule neurons are unique in that they only express γ-2.

*Address all correspondence to: Roger A. Nicoll, Department of Cellular and Molecular Pharmacology, University of California San Francisco, CA 94143, Phone: (415) 476-2018, nicoll@cmp.ucsf.edu.

Accordingly, cultured granule neurons from the mutant mouse *stargazer*, which lack functional γ-2 protein, have been used as a model system to understand TARP function (Chen et al., 2000; Cho et al., 2007; Milstein et al., 2007). Loss of γ-2 in these cells abolishes surface and synaptic AMPAR expression (Chen et al., 2000; Hashimoto et al., 1999). Similar phenotypes result from the loss of TARP family members in other neuronal cell types as well (Menuz et al., 2008; Rouach et al., 2005). Therefore, TARPs are believed to be necessary for AMPAR membrane trafficking and synaptic targeting throughout the brain.

An important unanswered question in the field concerns the stoichiometry of the association between TARPs and AMPARs. We previously demonstrated that the decay kinetics of synaptic AMPARs varies with the expression level of TARP γ-2 in cerebellar granule neurons, suggesting a variable TARP/AMPAR stoichiometry (Milstein et al., 2007). However, it was not possible to determine the exact stoichiometry from these data; the result could have been produced by mixed populations of AMPARs with anywhere from zero to four associated TARPs. To address whether a variable number of TARPs can assemble with AMPARs, one needs a technique that allows the number of TARPs on individual AMPARs to be counted unambiguously. To this end we have constructed fusion proteins between GluA subunits and TARPs. By co-expressing in HEK cells combinations of GluA1 and GluA2 with and without fused TARPs, we have succeeded in titrating the number of TARPs bound to AMPARs, producing functional AMPAR complexes with zero, two, and four bound TARPs. Importantly, the relative efficacy of the partial agonist kainate, which is known to increase with TARP association (Tomita et al., 2005; Turetsky et al., 2005), proved to be a particularly sensitive measure of TARP/AMPAR stoichiometry. When compared with these expression data, the efficacy of kainate on endogenous AMPARs from hippocampal neurons is consistent with the binding of multiple TARPs per native AMPAR. Furthermore, relative differences in TARP expression levels produce different TARP/AMPAR stoichiometries in two different neuronal cell types, CA1 pyramidal neurons and dentate gyrus granule neurons. Finally, we found that, in addition to kainate efficacy, deactivation and desensitization kinetics of AMPARs vary with TARP expression levels in CA1 pyramidal neurons. This variation in stoichiometry broadens the ways in which TARPs modulate AMPAR function in the brain.

Results

1. Kainate efficacy is enhanced by fusion or co-expression of GluA1 and γ-2

To fix the number of TARPs associated with individual AMPARs, we fused the full length GluA1 to the N-terminus of TARP γ-2 with a short linker sequence (Figure 1A1). If these receptors assemble and form functional channels expressed on the cell surface, they will contain four TARPs. When expressed in HEK cells, outside-out patches containing the fusion construct A1γ-2 produced sizeable currents in response to application of 1 mM glutamate (Figure 1A2), demonstrating that these channels are properly folded, traffic to the plasma membrane, and appropriately gate in response to glutamate. In order to determine whether the fused TARP molecules are *functionally* associated with the AMPAR channel, we took advantage of the fact that TARP association increases the efficacy of the partial agonist, kainate (Tomita et al., 2005; Turetsky et al., 2005). Indeed, A1γ-2 (Figures 1B and 1H) responded to 1 mM kainate application with substantially larger currents than those produced by GluA1 alone (Figure 1C and H), demonstrating that the fused TARP molecules interact with the AMPAR channel and modulate the efficacy of kainate. In fact, A1γ-2 produced a similar increase in the kainate to glutamate ratio (I_{KA}/I_{Glu}), a measure of kainate efficacy, as co-expression of non-fused GluA1 with TARP γ-2 (Figures 1D and 1H). We also measured the kainate efficacy of channels produced by fusion of GluA1 with the other TARP family members, γ-3, γ-4, and γ-8. Each of these fusion constructs, A1γ-3 (Figure

1E), A1γ-4 (Figure 1F), and A1γ-8 (Figure 1G) produced indistinguishable kainate efficacies (Figure 1H). While some previous studies co-expressing GluAs and TARPs showed differences in kainate efficacy for different TARPs (Cho et al., 2007; Korber et al., 2007; Kott et al., 2007; Tomita et al., 2005), no difference was seen in kainate efficacy across TARPs expressed in *stargazer* cerebellar granule neurons (Milstein et al., 2007). Furthermore, we found in this set of experiments that the I_{KA}/I_{Glu} observed in HEK cells was sensitive to the ratio of co-transfected GluA and TARP cDNA, with saturating kainate efficacy requiring an GluA:TARP ratio of 1:5 for TARP γ-8 (Figure S1).

2. Kainate efficacy co-varies with TARP/AMPAR stoichiometry

The observation that fusion of AMPARs and TARPs produces an enhanced kainate efficacy comparable to co-expression of the non-fused proteins raises the possibility that the channels formed in the latter condition normally contain four TARP molecules. However, it is also possible that fewer than four TARPs are sufficient to saturate the effect of TARPs on kainate efficacy. To address this possibility, we devised a method to measure the properties of AMPARs that contain less than four TARP molecules. While AMPARs that do not contain the GluA2 subunit are readily blocked by the polyamine toxin philanthotoxin-433 (PhTx), those that do contain GluA2 are not. We reasoned that co-expression of A1γ-2 with non-fused GluA2 would produce two populations of channels – those containing only GluA1 with four TARPs, and those incorporating GluA2 and therefore containing fewer than four TARPs. By including a concentration of PhTx (600 nM) that blocks essentially all A1γ-2 receptors (Figure S2), we could block any four TARP channels and measure the kainate efficacy of the isolated population of GluA2-containing AMPARs with fewer than four associated TARPs. Co-expression of A1γ-2 with GluA2 (Figure 2C), as well as the converse, GluA1+A2γ-2 (Figure 2D), produced kainate efficacies close to halfway between that of GluA1+GluA2, which contains no TARPs (Figure 2A) and A1γ-2+A2γ-2, which contains four TARPs (Figure 2B). This establishes unambiguously that AMPAR channels can be formed that contain fewer than four TARP molecules, and that kainate efficacy co-varies with TARP/AMPAR stoichiometry. We obtained similar results with fusion constructs between GluAs and TARP γ-8, with four TARP channels producing maximal kainate efficacy (Figure 2F), and channels associated with less than four TARPs producing roughly half the maximal kainate efficacy (Figure 2G and H). In summary, functional AMPARs can be produced that contain zero or four TARP molecules and, in addition, receptors can form with an intermediate stoichiometry (Figure 2I). This establishes that kainate efficacy can be used to distinguish between AMPARs with variable TARP/AMPAR stoichiometries.

What is the exact stoichiometry of the populations containing less than four TARPs? The finding that these heteromers formed by co-expression of GluAs with and without tethered TARPs produce kainate efficacies intermediate between zero-TARP and four TARP channels, suggests that they may contain two TARPs. If there is an absolute requirement that heteromeric AMPARs contain two GluA1s and two GluA2s when they are co-expressed in vitro (Mansour et al., 2001), then all of the heteromers would contain precisely two TARPs. If, on the other hand, GluA1 and GluA2 assemble randomly (Washburn et al., 1997), then co-expression of equal amounts of A1γ-2 and GluA2 would produce channels that predominantly contain two GluA2 subunits, but channels with other stoichiometries would also be present. To distinguish between these possibilities, we varied the ratio of co-expressed A1γ-2 and GluA2 cDNA in order to bias the assembly of AMPARs towards channels that contain either one or three GluA2s, and therefore three or one TARPs, respectively. To verify that altering the ratio of co-transfected cDNAs actually results in surface expression of AMPARs with the expected subunit compositions, we measured the percent block by PhTx of glutamate-evoked currents in outside-out patches. When A1γ-2

was expressed in 20-fold excess of GluA2, PhTx blocked ~90%, while the converse expression ratio produces negligible block by PhTx, as predicted by either model of assembly (Figure S3A).

Having confirmed that our co-transfection conditions indeed vary the subunit composition of surface expressed AMPARs, we next isolated the GluA2-containing, heteromeric AMPAR populations with PhTx and determined their kainate efficacies. When expressing 20-fold more A1γ-2 than GluA2, random assembly would produce heteromeric channels that contain at most one GluA2 subunit, and therefore three TARPs, while assembly that prefers heterodimers would produce channels that contain predominantly two GluA2 subunits, and therefore two TARPs (Figure S3B). Consistent with the latter model, we found that the kainate efficacy for this condition was identical to that obtained with a transfection ratio of 3:2 (Figure 2J). Similar results were obtained in the converse experiment expressing 20-fold more GluA2 than A1γ-2 (Figure 2J). In this case, channels containing four GluA2s and zero TARPs produce negligible currents due to deficits in trafficking and low conductance (Burnashev et al., 1992; Hollmann and Heinemann, 1994). Indeed, in our conditions homomeric GluA2 receptors generated essentially no current. The slight decrease in kainate efficacy observed for this condition is intermediate between the values predicted by the two assembly models (Figure S3B). This suggests that under these extreme conditions, when GluA2 expression greatly exceeds that of GluA1, it is possible for some channels to form that contain three GluA2 subunits, but assembly is still strongly biased towards formation of channels containing two GluA2 subunits. Comparison of the experimental data to values predicted by various assembly models further rules out the potential complication that kainate efficacy could be saturated for AMPARs containing fewer than four bound TARPs (Figure S3B). These experiments strongly suggest that, even under conditions that should favor channels with assembly ratios of 1:3 or 3:1, GluA1 and GluA2 preferentially assemble at a ratio of 2:2, and that the intermediate kainate efficacy observed when co-expressing GluAs with and without fused TARPs reflects receptors that predominantly contain two TARPs.

For experiments co-expressing GluA1+A2γ-2, we expressed GluA1 in excess (3:2) to minimize the chance of forming A2γ-2 homomers, since there is no available pharmacology to block these receptors. Under these conditions, 600 nM PhTx blocked 36±8.3% (n = 7) of the glutamate currents (Figure S2D), indicating the presence of GluA1 homomers in the plasma membrane. In the presence of PhTx, the KA/Glu ratio was 0.29±0.03 (n = 9, Figure 2D, H), again suggesting the remaining heteromers contained two TARPs.

If co-expression of GluA1 and GluA2 results in preferential formation of heterodimers, we wondered if by just co-expressing fused and non-fused GluA2 we could force the assembly of channels that contain only one TARP. By co-expressing GluA2 in excess of A2γ-2, we predicted that random assembly would prevail, producing either GluA2 homomers containing zero TARPs that do not traffic or conduct, or channels that incorporated one A2γ-2 that could be assayed for kainate efficacy. First we confirmed that expression of A2γ-2 on its own results in a high KA/Glu ratio similar to A1γ-2 (0.52±0.04, n = 7), consistent with a four TARP receptor. Second, we confirmed that expression of GluA2 did not produce currents in our conditions. Surprisingly, when A2γ-2 and GluA2 are expressed with a 1:20 ratio, the resulting KA/Glu ratio (0.38±0.02, n = 7) is substantially larger than would be expected for a one TARP receptor. This suggests that either GluA2 homomers containing one TARP are not assembled, or they are unable to traffic or conduct, similar to GluA2 homomers expressed in the absence of TARPs.

3. TARP stoichiometry differs between two distinct types of hippocampal neurons

We sought to determine if the above results from HEK cells could be compared with data from native AMPARs in neurons in order to read out native TARP/AMPAR stoichiometry. First we measured the kainate efficacy of AMPARs in outside-out patches from mouse CA1 pyramidal neurons. These AMPARs are predominantly (95%) GluA1/2 heteromers (Lu et al., 2009; Zamanillo et al., 1999) associated with TARP γ-8 (Rouach et al., 2005; Tomita et al., 2003), and therefore can be directly compared to the data we obtained expressing these GluAs with TARP γ-8. These native AMPARs displayed a high kainate efficacy consistent with incorporation of four TARP molecules per AMPAR complex (Figure 3A1 and C). However, while we examined only the *flip* splice variant of AMPARs in HEK cells, CA1 pyramidal neurons express both *flip* and *flop* variants of AMPARs (Monyer et al., 1991). To determine if this might affect the comparison, we repeated the experiments in CA3 pyramidal neurons, which have been shown to express predominantly *flip* variants (Monyer et al., 1991). These experiments yielded a KA/Glu ratio identical to those obtained in CA1 pyramidal neurons (0.47±0.04, n = 11), indicating that even if *flop* receptors exist in CA1 pyramidal neurons, they do not substantially alter kainate efficacy under our conditions. Furthermore, inclusion of the compound PEPA, a drug that blocks the desensitization of *flop* AMPARs (Sekiguchi et al., 1998), especially when associated with TARPs (Tomita et al., 2006), had no effect on glutamate responses in CA1 pyramidal neurons (Figure S5).

We further wondered if TARP/AMPAR stoichiometry could be altered by genetic depletion or exogenous over-expression of TARPs. Indeed, outside-out patches from TARP γ-8 (+/−) (Figure 3A2 and C) and (−/−) (Figures 3A3 and 3C) mice revealed reduced kainate efficacy. However, over-expression of either TARP γ-8 (Figures 3A4 and 3C) or TARP γ-2 (I_{KA}/I_{Glu} = 0.53±0.03; n = 4, data not shown) did not substantially increase kainate efficacy, supporting the notion that native AMPARs in CA1 pyramidal neurons are normally saturated by TARP expression, and therefore contain four TARPs per AMPAR complex. The finding that over-expression of TARP γ-2 does not alter kainate efficacy differs from the results of (Turetsky et al., 2005). However, these authors specifically used immature neurons in which TARP expression levels are low, likely containing AMPARs with reduced stoichiometry.

These data are in striking contrast to our previous findings from cerebellar granule neurons, where the apparent TARP/AMPAR stoichiometry was not saturated in wild-type neurons (Milstein et al., 2007), and could be increased by over-expression of TARP γ-2. This raises the possibility that TARP/AMPAR stoichiometry is a parameter that differs across neuronal cell types. We tested this possibility by measuring kainate efficacy in another neuronal population, hippocampal dentate gyrus granule cells. *In situ* data suggests that these neurons express lower levels of TARP γ-8 than CA1 or CA3 pyramidal neurons (Lein et al., 2007), and might be expected to display reduced TARP/AMPAR stoichiometry. Indeed, wild-type granule cells exhibited a lower kainate efficacy than that observed in CA1 pyramidal cells (Figures 3B1 and 3C). Furthermore, exogenous over-expression of TARP γ-8 substantially increased kainate efficacy in these cells (Figures 3B4 and 3C), confirming that AMPARs are not saturated with TARPs in this cell type. Importantly, the kainate efficacy observed when TARP γ-8 was overepressed was identical to that recorded in CA1 pyramidal neurons, strongly implying that the pharmacological property of AMPARs in granule cells are the same as in CA1 pyramidal neurons. Similar to pyramidal neurons, genetic depletion of TARP γ-8 further reduced kainate efficacy, with γ-8 (+/−) (Figures 3B2 and 3C) and γ-8 (−/−) (Figures 3B3 and 3C) mice exhibiting reduced kainate efficacy relative to wild-type.

In this study we chose to use kainate efficacy as an assay to probe the influence of TARP association on AMPAR function, because of its ease and high sensitivity. However, more physiologically relevant parameters of AMPAR function are the kinetics of channel

deactivation and desensitization, which are known to be influenced by TARP association (Priel et al., 2005; Tomita et al., 2005; Turetsky et al., 2005). We therefore conducted experiments in CA1 pyramidal neurons from TARP γ-8 mutant mice using fast application of glutamate to outside-out patches. The time course of deactivation in control mice was similar to that previously reported for rat neurons (Spruston et al., 1995) (Figure 3D). However, in TARP γ-8 (−/−) mice, AMPAR deactivation is significantly faster, and it was intermediate in heterozygous TARP γ-8 (+/−) mice (Figure 3D). The time course of AMPAR desensitization similarly varied with TARP expression level (Table S1).

Discussion

Since the discovery of TARPs a decade ago, numerous studies have established that these auxiliary subunits control the trafficking and gating of AMPARs, and that the magnitude of this effect depends on the specific TARP subtype (Cho et al., 2007; Kott et al., 2007; Milstein et al., 2007). Might the number of TARP molecules that associate with individual AMPAR channels also regulate gating? Although previous data raise this possibility (Milstein et al., 2007), resolving TARP/AMPAR stoichiometry has been surprisingly difficult. We have genetically linked TARPs to AMPARs and have thus been able to identify the number of TARPs associated with native AMPARs.

By expressing AMPAR subunits covalently linked to TARPs in HEK cells we have compared the properties of AMPARs containing zero or four TARPs and receptors with an intermediate stoichiometry. We show that kainate efficacy, previously shown to increase with TARP association (Tomita et al., 2005; Turetsky et al., 2005), varies with TARP/AMPAR stoichiometry and can be used to distinguish between AMPARs that are saturated or unsaturated by TARP expression. The functional effects of TARPs γ-2 and γ-8 on fused GluA1 and GluA2 were similar, and both varied with TARP/AMPAR stoichiometry. These results not only establish that AMPARs can assemble with different numbers of TARPs, but also provide valuable quantitative data that can be compared to native AMPARs in neurons. Although not addressed in this study, it would not be surprising if the magnitude of other modulatory effects of TARPs, such as the sensitivity of Ca^{2+}-permeable AMPARs to block by intracellular polyamines (Soto et al., 2007), and the trafficking of AMPARs to synapses, might be similarly regulated by stoichiometry.

When we expressed heteromeric receptors in which only one of the subunits was tethered to a TARP we consistently obtained receptors with a kainate efficacy that was roughly intermediate between that observed with zero-TARP and four TARP receptors. This finding is consistent with the model in which AMPARs are assembled with a stoichiometry of two GluA1 and two GluA2 subunits (Mansour et al., 2001). If, however, subunits can randomly assemble with a variable subunit stoichiometry (Washburn et al., 1997), then the intermediate kainate efficacy could represent a mixed population of heteromers with receptors containing two TARPs predominating. Another possible interpretation of our results is that the kainate efficacy actually saturates when less than four TARPs are bound to the receptor. Although this would not alter the conclusion that stoichiometry can vary, it would question the quantitative conclusions. However, a simple set of calculations that predicts the kainate efficacies of AMPARs that are produced by varying models of channel assembly (Figure S3B) supports the scenario in which heterodimer formation is preferred and the ratio saturates at four TARPs.

Remarkably, we find that AMPARs in CA1 pyramidal neurons are normally associated with four molecules of TARP γ-8. When the expression level of γ-8 is reduced, the number of TARPs associated with each AMPAR is reduced. At this point we can only speculate as to what the precise TARP/AMPAR stoichiometry is in γ-8 (−/−) and γ-8 (+/−) mice. If we

assume that at least one TARP must be associated with AMPARs in order for them to be efficiently trafficked to the cell surface, then we would expect all surface receptors to contain at least one TARP; indeed, the observed kainate efficacy of γ-8 (−/−) pyramidal neurons was between that expected for zero and two TARPs, indicating that perhaps it is just one TARP. In this scenario, TARPs γ-2 and γ-3, which are also expressed in pyramidal neurons (Lein et al., 2007; Tomita et al., 2003), are associated with the remaining AMPARs in γ-8 (−/−) neurons. In addition, we demonstrate in CA1 neurons the time course of AMPAR deactivation and desensitization varies with γ-8 expression level, consistent with the change of TARP/AMPAR stoichiometry.

Furthermore, we find that TARP/AMPAR stoichiometry differs between distinct neuronal cell types. Unlike CA1 pyramidal neurons, hippocampal dentate gyrus granule cells are not saturated with four TARPs, but instead appear to express a mixed population of AMPARs containing fewer than four TARPs. This is also consistent with the data we previously acquired from cerebellar granule neurons (Milstein et al., 2007), and reinforces the notion that differences in the expression level of different TARP subtypes diversifies the functional properties of neuronal AMPARs, not only through subtype-specific regulation, but also through variable TARP/AMPAR stoichiometries.

Methods and materials

1. cDNA and constructs

cDNAs of γ-2, γ-3, γ-4, and γ-8 and flip-type GluA1 and GluA2 were used in current study. The cDNAs were constructed into two vectors: pIRES2-EGFP and pIRES2-dsRed (Clontech). GluA1 and all TARPs were subcloned with EcoR 1 and Sal 1 sites (Milstein et al., 2007). GluA2 was inserted with Xho 1 and Sal 1 sites. A Kozak sequence was engineered in front of the start codon. To construct A1γ-2, the following primers were used: forward primer, 5′-GATCTCGAGCTCGCCACCATGCCGTAC-3′; reverse primer, 5′-CCCGAATTCCTGTTGCTGTTGCTGTTGCTGTTGCTGTTGCAATCCTGTGGCTCC-3′. Standard PCR was carried out with the GluA1 template and the product was inserted into γ-2 containing pIRES2 vectors with Xho1 and EcoR1 site, thus fusing GluA1 to the N-terminus of γ-2 with a short linker sequence $(Q)_{10}$EFAT. A1γ-8, A1γ-3, A1γ-4 were constructed similarly. The primers used in constructing A2γ-2 and A2γ-8 were as follows: forward primer, 5′-GGACGCTAGCGCCACCATGCAAAAGATTATGC-3′; reverse primer, 5′-GAGCTCGAGGACTGTTGCTGTTGCTGTTGAATTTTAACACTCTCGATGCC-3′. Nhe1 and Xho1 were used to insert the PCR product. The linker sequence used between GluA2 and TARPs was $(Q)_6(S)_5$FEFAT. The constructs were verified with sequencing (Elim). EGFP and/or dsRed fluorescence allowed visualization of co-expression. Indeed, co-expression was observed in more than 90% of the positive transfected cells.

2. HEK293T cell culture and transfection

HEK293T cells were used for expression of GluAs, TARPs and fusion constructs. HEK293T cells were cultured in a 37°C incubator sup plied with 5% CO_2 (Milstein et al., 2007). Transfection was performed in 35mm dishes or 6-well plates with above cDNAs using lipofectomine™2000 reagents according to the protocol provided by the manufacturers (Invitrogen). The following strategies were used in transfection if not otherwise specified. Total cDNA used for transfection per 35mm dish or per well in 6-well plates was 0.5 μg. When expression was carried out, a 2:3 ratio of GluA to TARP cDNA was used, except for A1+γ-8, where 0.2 μg GluA1 and 5X or 10X γ-8 were used. When GluA1 (or fusion construct) and GluA2 (or fusion construct) were co-expressed, GluA1:GluA2 was 3:2. Transfection was terminated in 2–3 hours. Cells were dissociated with 0.05% trypsin and

plated on coverslips pretreated with poly-D-lysine. Recording was performed 24–48 hours after transfection. The amplitude of glutamate evoked currents varied considerably among HEK cells. To determine if the amplitude of the glutamate current, which is presumably due primarily to the number of receptors on the surface, had any effect on the KA/Glu ratio we plotted the size of the glutamate current against the size of the kainate current. The KA/Glu ratio was entirely independent of the magnitude of the glutamate evoked current. (Figure S4).

3. Acute hippocampus slices and slice cultures

Transverse hippocampal slices 300 μm thick were cut from p14–p23 mice on a Leica vibratome in cutting solution containing (in mM): NaCl 50, KCl 2.5, $CaCl_2$ 0.5, $MgCl_2$ 7, NaH_2PO_4 1.0, $NaHCO_3$ 25, glucose 10 and sucrose 150. Freshly cut slices were placed in an incubating chamber containing artificial cerebrospinal fluid (ACSF), containing (in mM) NaCl 119, KCl 2.5, $NaHCO_3$ 26, Na_2PO_4 1, glucose 11, $CaCl_2$ 4, $MgCl_2$ 4 and recovered at 35 °C for ~1h. Slices were then maintained in ACSF at room temperature prior to recording. After 0.5–1 h of incubation at room temperature, slices were transferred to a submersion chamber on an upright Olympus microscope. All solutions were saturated with 95% O_2/5% CO_2. CA1 pyramidal cells were visualized by Infrared differential interference contrast microscopy. Cultured slices were prepared and transfected as previously described (Schnell et al., 2002). Briefly, hippocampi were dissected from P6–P9 mice and transfected with γ-8-IRES-EGFP using biolistic gene fransfer after 2–3 days in culture. Slices were cultured for an additional 2–7 days before recording.

4. Electrophysiology

Out-side out patches were excised from transfected HEK293T cells or hippocampal neurons in acute slices or slice cultures. Coverslips with transfected HEK cells were maintained during recording with external solution containing (in mM): NaCl 140, KCl 5, $MgCl_2$ 1.4, EGTA 5, HEPES 10, NaH_2PO_4 1, D-glucose 10 and NBQX 0.01 and pH adjusted to 7.4. Outside-out patches were excised from positively transfected cells identified by epifluorescence microscopy with 3 to 5 M3 borosilicate glass pipettes. The internal solution contained (in mM): CsF 135, CsOH 33, $MgCl_2$ 2, $CaCl_2$ 1, EGTA 11, HEPES 10, spermine 0.1 with pH adjusted to 7.2. The glutamate and kainate induced currents were recorded while holding the patches at −70mV. Glutamate (1 mM) and kainate (1 mM) were applied to patches in extracellular solution containing (in mM): NaCl 150, KCl 2.5, HEPES 10, glucose 10, $CaCl_2$ 4, $MgCl_2$ 4, Cyclothiazide 0.1, pH 7.4. In addition, when GluA1/A2 channels with and without TARPs were studied, 600 nM or 10 μM PhTx was included to block the potential GluA1 homomeric channels (Figure S2). The hippocampal slices (acute or culture) were perfused with ACSF bubbled with 5% CO_2 and 95% O_2. In slice cultures, the cells with γ-8 over-expression were visualized with EGFP fluorescence. Patches were excised from CA1 pyramidal neurons and dentate granule cells. The currents were recorded with pipette solution containing: $CsMeSO_4$ 135, NaCl 8, Hepes 10, Na_3GTP 0.3, MgATP 4, EGTA 0.3, QX-314 5, and spermine 0.1. Glutamate and kainate were similarly dissolved in extracellular solution with the addition of 100 μM picrotoxin, 100 μM D-APV and 500 nM tetrodotoxin to isolate AMPAR-mediated current. In fast application experiments, the above extracellular solution (without cyclothiazide) was used for control and glutamate dilution. Data were collected with an Axopatch 1D amplifier (Axon Instruments, Foster City, CA), filtered at 2 kHz, digitized at 10 kHz for most patches and at 50 kHz for the fast application. Analysis of deactivation and desensitization was described in a previous study (Milstein et al., 2007). Data were presented as mean ± SEM. Differences in means were tested with the ANOVA or Student t test and were accepted as significant if $p \leq 0.05$

Supplementary Material

Refer to Web version on PubMed Central for supplementary material.

Acknowledgments

We thank Kirsten Bjorgan for preparing hippocampal slice cultures and all of the members of the R.A.N. laboratory for helpful discussions. We also thank Geoffrey Kerchner for critical reading on the manuscript. R.A.N. is supported by grants from the National Institutes of Health. W.L. is supported by a postdoctoral fellowship from the American Heart Association. A.D.M. is supported by a Graduate Research Fellowship from the National Science Foundation.

References

Burnashev N, Monyer H, Seeburg PH, Sakmann B. Divalent ion permeability of AMPA receptor channels is dominated by the edited form of a single subunit. Neuron. 1992; 8:189–198. [PubMed: 1370372]

Chen L, Chetkovich DM, Petralia RS, Sweeney NT, Kawasaki Y, Wenthold RJ, Bredt DS, Nicoll RA. Stargazin regulates synaptic targeting of AMPA receptors by two distinct mechanisms. Nature. 2000; 408:936–943. [PubMed: 11140673]

Cho CH, St-Gelais F, Zhang W, Tomita S, Howe JR. Two families of TARP isoforms that have distinct effects on the kinetic properties of AMPA receptors and synaptic currents. Neuron. 2007; 55:890–904. [PubMed: 17880893]

Collingridge GL, Olsen RW, Peters J, Spedding M. A nomenclature for ligand-gated ion channels. Neuropharmacology. 2008

Dingledine R, Borges K, Bowie D, Traynelis SF. The glutamate receptor ion channels. Pharmacol Rev. 1999; 51:7–61. [PubMed: 10049997]

Hashimoto K, Fukaya M, Qiao X, Sakimura K, Watanabe M, Kano M. Impairment of AMPA receptor function in cerebellar granule cells of ataxic mutant mouse stargazer. J Neurosci. 1999; 19:6027–6036. [PubMed: 10407040]

Hollmann M, Heinemann S. Cloned glutamate receptors. Annu Rev Neurosci. 1994; 17:31–108. [PubMed: 8210177]

Korber C, Werner M, Kott S, Ma ZL, Hollmann M. The transmembrane AMPA receptor regulatory protein gamma4 is a more effective modulator of AMPA receptor function than stargazin (gamma2). J Neurosci. 2007; 27:8442–8447. [PubMed: 17670991]

Kott S, Werner M, Korber C, Hollmann M. Electrophysiological properties of AMPA receptors are differentially modulated depending on the associated member of the TARP family. J Neurosci. 2007; 27:3780–3789. [PubMed: 17409242]

Lein ES, Hawrylycz MJ, Ao N, Ayres M, Bensinger A, Bernard A, Boe AF, Boguski MS, Brockway KS, Byrnes EJ, et al. Genome-wide atlas of gene expression in the adult mouse brain. Nature. 2007; 445:168–176. [PubMed: 17151600]

Lu W, Shi Y, Jackson AC, Bjorgan K, During MJ, Sprengel R, Seeburg PH, Nicoll RA. Subunit composition of synaptic AMPA receptors revealed by a single-cell genetic approach. Neuron. 2009; 62:254–268. [PubMed: 19409270]

Mansour M, Nagarajan N, Nehring RB, Clements JD, Rosenmund C. Heteromeric AMPA receptors assemble with a preferred subunit stoichiometry and spatial arrangement. Neuron. 2001; 32:841–853. [PubMed: 11738030]

Mayer ML, Armstrong N. Structure and function of glutamate receptor ion channels. Annu Rev Physiol. 2004; 66:161–181. [PubMed: 14977400]

Menuz K, O'Brien JL, Karmizadegan S, Bredt DS, Nicoll RA. TARP redundancy is critical for maintaining AMPA receptor function. J Neurosci. 2008; 28:8740–8746. [PubMed: 18753375]

Milstein AD, Nicoll RA. Regulation of AMPA receptor gating and pharmacology by TARP auxiliary subunits. Trends Pharmacol Sci. 2008; 29:333–339. [PubMed: 18514334]

Milstein AD, Zhou W, Karimzadegan S, Bredt DS, Nicoll RA. TARP subtypes differentially and dose-dependently control synaptic AMPA receptor gating. Neuron. 2007; 55:905–918. [PubMed: 17880894]

Monyer H, Seeburg PH, Wisden W. Glutamate-operated channels: developmentally early and mature forms arise by alternative splicing. Neuron. 1991; 6:799–810. [PubMed: 1673851]

Nicoll RA, Tomita S, Bredt DS. Auxiliary subunits assist AMPA-type glutamate receptors. Science. 2006; 311:1253–1256. [PubMed: 16513974]

Osten P, Stern-Bach Y. Learning from stargazin: the mouse, the phenotype and the unexpected. Curr Opin Neurobiol. 2006; 16:275–280. [PubMed: 16678401]

Priel A, Kolleker A, Ayalon G, Gillor M, Osten P, Stern-Bach Y. Stargazin reduces desensitization and slows deactivation of the AMPA-type glutamate receptors. J Neurosci. 2005; 25:2682–2686. [PubMed: 15758178]

Rouach N, Byrd K, Petralia RS, Elias GM, Adesnik H, Tomita S, Karimzadegan S, Kealey C, Bredt DS, Nicoll RA. TARP gamma-8 controls hippocampal AMPA receptor number, distribution and synaptic plasticity. Nat Neurosci. 2005; 8:1525–1533. [PubMed: 16222232]

Schnell E, Sizemore M, Karimzadegan S, Chen L, Bredt DS, Nicoll RA. Direct interactions between PSD-95 and stargazin control synaptic AMPA receptor number. Proc Natl Acad Sci U S A. 2002; 99:13902–13907. [PubMed: 12359873]

Seeburg PH. The TINS/TiPS Lecture. The molecular biology of mammalian glutamate receptor channels. Trends Neurosci. 1993; 16:359–365. [PubMed: 7694406]

Sekiguchi M, Takeo J, Harada T, Morimoto T, Kudo Y, Yamashita S, Kohsaka S, Wada K. Pharmacological detection of AMPA receptor heterogeneity by use of two allosteric potentiators in rat hippocampal cultures. Br J Pharmacol. 1998; 123:1294–1303. [PubMed: 9579722]

Soto D, Coombs ID, Kelly L, Farrant M, Cull-Candy SG. Stargazin attenuates intracellular polyamine block of calcium-permeable AMPA receptors. Nat Neurosci. 2007; 10:1260–1267. [PubMed: 17873873]

Spruston N, Jonas P, Sakmann B. Dendritic glutamate receptor channels in rat hippocampal CA3 and CA1 pyramidal neurons. J Physiol. 1995; 482(Pt 2):325–352. [PubMed: 7536248]

Tomita S, Adesnik H, Sekiguchi M, Zhang W, Wada K, Howe JR, Nicoll RA, Bredt DS. Stargazin modulates AMPA receptor gating and trafficking by distinct domains. Nature. 2005; 435:1052–1058. [PubMed: 15858532]

Tomita S, Chen L, Kawasaki Y, Petralia RS, Wenthold RJ, Nicoll RA, Bredt DS. Functional studies and distribution define a family of transmembrane AMPA receptor regulatory proteins. J Cell Biol. 2003; 161:805–816. [PubMed: 12771129]

Tomita S, Sekiguchi M, Wada K, Nicoll RA, Bredt DS. Stargazin controls the pharmacology of AMPA receptor potentiators. Proc Natl Acad Sci U S A. 2006; 103:10064–10067. [PubMed: 16785437]

Turetsky D, Garringer E, Patneau DK. Stargazin modulates native AMPA receptor functional properties by two distinct mechanisms. J Neurosci. 2005; 25:7438–7448. [PubMed: 16093395]

Washburn MS, Numberger M, Zhang S, Dingledine R. Differential dependence on GluR2 expression of three characteristic features of AMPA receptors. J Neurosci. 1997; 17:9393–9406. [PubMed: 9390995]

Zamanillo D, Sprengel R, Hvalby O, Jensen V, Burnashev N, Rozov A, Kaiser KM, Koster HJ, Borchardt T, Worley P, et al. Importance of AMPA receptors for hippocampal synaptic plasticity but not for spatial learning. Science. 1999; 284:1805–1811. [PubMed: 10364547]

Ziff EB. TARPs and the AMPA Receptor Trafficking Paradox. Neuron. 2007; 53:627–633. [PubMed: 17329203]

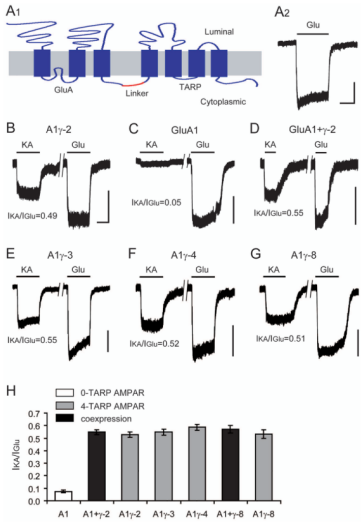

Figure 1.

Kainate efficacy is enhanced by co-expression or fusion of TARPs with GluA1. **A_1**. Construction of GluA-TARP fusion proteins. The full length GluA was fused to N-terminus of TARPs with a short segment of linker sequence. **A_2**.Glutamate (Glu, 1 mM) induced currents in an outside-out patch excised from an HEK293T cell transfected with GluA1 fused to TARP γ-2 (A1γ-2), indicating that this construct forms functional channels. The currents were recorded in presence of 100 μM of cyclothiazide. **B.** Kainate (KA, 1 mM) and glutamate (Glu, 1 mM) induced currents in an outside-out patch excised from a cell transfected with A1γ-2. On the sample patch, kainate induced current was 49% of that of glutamate. The kainate to glutamate ratio (I_{KA}/I_{Glu}) is referred to as the kainate efficacy. **C.** When cells were transfected with only GluA1 (A1), kainate induced currents were 5% of that of glutamate in the sample patch. **D.** Coexpression of GluA1 and γ-2 produced a similar kainate efficacy to that of the fusion protein A1γ-2. **E–G.** KA efficacy was similar in fusion constructs A1γ-3, A1γ-4 and A1γ-8. Scale bar: 2 s, 100 pA. Between slashed lines was 11.5 second. **H.** Summary of kainate efficacy in GluA1 homomeric receptors with or without TARPs. GluA1, 7.4±1.1%, n = 10; GluA1+γ-2, 54.9±1.9%, n = 10; A1γ-2, 52.7±2.1%, n = 10; A1γ-3, 54.8±2.5%, n = 7; A1γ-4, 58.8±2.4%, n = 6; GluA1+γ-8, 57.1±3.0%, n = 8; A1γ-8, 53.1±3.5%, n = 9. In GluR1+γ-2 experiment, the DNA ratio used in transfection was GluA1: γ-2 = 2:3. In GluR1+γ-8 experiments, 2:3 DNA ratio appeared not sufficient to form saturating TARP/AMPA stoichiometry. The data used here were pooled from GluA1: γ-8 = 1:5 and 1:10 (Figure S1).

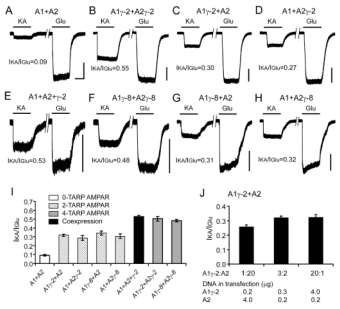

Figure 2.

Glutamate- and kainate-induced currents from GluA1/A2 receptors expressed in HEK293T cells. **A**–**H**, Examples of currents in outside-out patches. The cDNA of GluA1 with or without linked TARPs was over-numbering GluA2s (3:2). Scale bar: 2 s, 100 pA. **I**, Summary of kainate efficacy in GluA1/A2 receptors expressed in HEK cells. Note that without TARPs, GluA1/GluA2 had low kainate efficacy (A1+A2, 9.3±0.7%, n = 7). Fusion receptors containing four TARPs had increased kainate efficacy. A1γ-2+A2γ-2, 50.3±2.5%, n = 10; A1γ-8+A2γ-8, 48.2±1.5%, n = 8. Co-expression of TARP γ-2 with GluA1/A2 had high kainate efficacy (A1+A2+γ-2, 52.8±1.3%, n = 5). The KA efficacy was intermediate in 2-TARP channels. A1γ-2+A2, 31.8±1.3%, n = 9; A1+A2γ-2, 28.7±2.8%, n = 9; A1γ-8+A2, 34.3±2.1%, n = 7; A1+A2γ-8, 30.7±2.6%, n = 7. **J.** KA efficacy did not vary with variable ratio of A1γ-2 and GluA2 in co-expression. When A1γ-2 and GluA2 were co-transfected in a ratio of 20:1, KA efficacy (32.1±2.2%, n = 5) was not higher than that in a ratio of 3:2 (31.8±1.3%, n = 9). When A1γ-2 and GluA2 were expressed in a ratio of 1:20, KA efficacy was not significantly changed (25.6±1.5%, n = 8, p = 0.12 compared to 3:2 group). All currents in this figure were recorded in the presence of 100 μM cyclothiazide. PhTx (600 nM-10 **μ**M) was included in the solutions to isolate heteromeric GluA1/A2 channels.

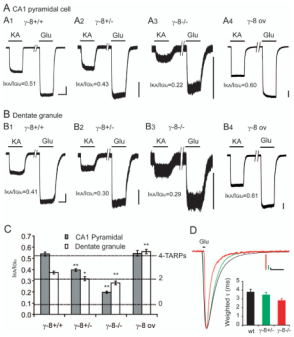

Figure 3.

Kainate efficacy in extrasynaptic AMPARs in hippocampus pyramidal neurons and dentate granule cells. **A.** Hippocampal CA1 pyramidal cells. **A_1**. WT animals, kainate induced currents were about half of that induced by glutamate. **A_2**. In TARP γ-8 heterozygote, the kainate efficacy was reduced. **A_3**. In γ-8 knockout mice the kainate efficacy was further reduced. **A_4**. A sample patch from γ-8 over-expression (γ-8 ov). Scale bar: 2 s, 100 pA. **B.** dentate granule cells. **$B_{1–4}$** Sample patches from granule cells in WT, γ-8 +/− and γ-8 −/− and in a cell over-expressing γ-8. Scale bar: 2 s, 50 pA. **C**. Summary of I_{KA}/I_{Glu}. Pyramidal neurons: WT, 53.8±2.0%, n = 11; γ-8 +/−, 39.5±1.2%, n = 17; KO, 19.8±1.1%, n = 16; Over-expression, 54.5±2.5%, n = 8. Dentate granule neurons: WT, 37.3±1.4%, n = 13; γ-8 +/−, 31.7±1.8%, n = 11; γ-8 −/−, 27.9±1.6%, n = 10; Over-expression, 55.9±2.0%, n = 9. The dashed lines indicate the kainate efficacy of AMPA receptors expressed in HEK cells. Note that kainate efficacy in WT pyramidal neurons is identical to that of four TARP channels expressed in HEK cells, suggesting the TARP stoichiometry is saturated in this neuronal type. In contrast, kainate efficacy is drastically lower in dentate granule neurons, indicating the TARP stoichiometry is unsaturated in granule cells. Also note that kainate efficacy in γ-8 knockout neurons is still bigger than those of apo-AMPAR in HEK cells suggesting the remaining AMPARs are associated with non-γ-8 TARPs. *, $p<0.05$; ** $p<0.01$ compared to WT cells. **D.** Deactivation of AMPA receptors in outside-out patches pulled from CA1 pyramidal neurons. The patches were exposed to 1 mM glutamate for 1 ms. The displayed currents were average of 10–15 traces and peak scaled. Scale bar, 20 pA, 5 ms. The insert is the weighted τ of deactivation, which was slow in WT CA1 neurons (3.83±0.28 ms, n = 19), and significantly faster in γ-8 knockout neurons (2.82±0.21 ms, n = 14, $p<0.01$). An intermediate deactivation was seen in γ-8 heterozygous (3.49±0.26 ms, n = 18). The deactivation curves were well fit by a double exponential function, as shown in Table S1.